An electrohydrodynamic bioprinter for alginate hydrogels containing living cells

Luca Gasperini [1,2]

luca.gasperini@ing.unitn.it

Devid Maniglio [1,2,3]

devid.maniglio@ing.unitn.it

Antonella Motta [1,2,3]

antonella.motta@ing.unitn.it

Claudio Migliaresi [1,2,3]

claudio.migliaresi@ing.unitn.it

Contact info for each author: see 1) Corresponding author : Claudio Migliaresi

1) Department of Industrial Engineering, Biotech Research Center, University of Trento, Via delle Regole 101, 38123, Mattarello, Italy. Tel: +390461282765

2) European Institute of Excellence on Tissue Engineering and Regenerative Medicine, Trento, Italy.

3) INSTM - Consorzio Interuniveristario Nazionale per la Scienza e Tecnologia dei Materiali, via G. Giusti 9, 50121 Firenze, Italy.

Abstract

In this work we present a bioprinting technique that exploits the electrohydrodynamic process to obtain a jet of liquid alginate beads containing cells. A printer is used to microfabricate hydrogels block by block following a bottom up approach. Alginate beads constitute the building blocks of the

microfabricated structures. The beads are placed at predefined position on a target substrate made of calcium enriched gelatin, where they crosslink upon contact without the need of further post-processing. The printed sample can be easily removed from the substrate at physiological temperature. 3D printing is accomplished by the deposition of multiple layers of hydrogel. We have investigated the parameters influencing the process, the compatibility of the printing procedure with cells and their survival after printing.

1 Introduction

Bioprinting is a computer aided manufacturing technique that allows the construction of structures piece by piece using basic units called building blocks (1). A bioprinter is constituted of a computer aided positioning and deposition system, a bio-ink that feeds the deposition system and a bio-paper that acts as the substrate for the deposition. The computer controls the placing apparatus by moving the sample or the deposition heads along a predetermined path, initiating the deposition of the bio-ink when needed.

There is an increasing interest in using cell based bio-inks so that cells can be placed at predefined positions. In fact this approach raises new possibilities for a wide range of applications. It could be possible, for instance, to fabricate multiple cell constructs for the in vitro testing of pharmacological molecules, additives and contaminants, with more reliable results, faster response and reduced animal testing (2). Bioprinting, and its ability to place cells at specific space coordinates, has been also proposed as a mean to fabricate highly ordered cellular structures that could mimic the complexity of the natural tissue (3,4). However, even if this approach is fashionable and attractive, it is still at early development stage and its success in rebuilding fully functional complex living tissues block-by-block may be not easily reachable in a close future. Another interesting application of bioprinting, potentially in a closer future, is to manufacture cell-laden devices for the release of therapeutic molecules (5). In fact the bio-ink can be a hydrogel precursor containing cells and hydrogels could be microfabricated using cell-laden capsules or beads as building blocks. The capsules protect the cells by the host immune system so that xenogenic endocrine cells may be encapsulated and transplanted to threat diseases such as diabetes (6), anemia (7) and dwarfism (8). The devices could be designed to be easier to handle and transplant, compared with the single microcapsules. Moreover, they can be designed to optimize the exposure of

encapsulated cells to the surrounding fluids and, as such, the effectiveness of their response to the environmental clues.

Recently some groups have already proposed some bioprinters based on different deposition systems.

For example Xu et al. (9) reported the possibility to adapt commercial ink jet printers and print viable cells while Cui and Boland (10) with a similar printer, were able to print human microvascular endothelial cells on a fibrinogen substrate using a bio-ink made of cells and thrombin. With a laser printer, Barron et al. (11) used a forward transfer technique in which a laser is used to move cells from a biological medium to a receiving substrate, while Ringeisen et al. (12) printed pluripotent embryonal carcinoma cells with minimal single-strand DNA damage. These systems have been proven to be valid in specific situations; however a high throughput deposition system, with good spot resolution and a high load volume able to print samples in 3D is still missing (13).

An optimal deposition system should allow a controlled ejection of undamaged cells travelling for a relative short distance before reaching the target substrate, it should be high throughput and, possibly, inexpensive. The electro hydro dynamic jetting (EHDJ) technology can fulfill these requirements. Moreover with EHDJ it is possible to create micrometric size beads and the bio-ink is supplied by a programmable automatic syringe, giving a wide range of loading options (14).

In electro hydro dynamic systems a solution is fed through a positively charged metallic needle. The solution reacts to the presence of the charge, generating repulsive coulombic forces on its surface, causing the deformation of the meniscus at the tip of the needle into a Taylor cone (15). If the voltage is high enough, the electrostatic repulsion on the surface can overcome the surface tension at the apex of the liquid cone, leading to its disintegration (Rayleigh limit) and creating a jet of drops (16). The process is governed by parameters that can be easily changed, some of them even without interrupting the deposition system (voltage, flux of solution, distance from target), possibly leading to different geometric shapes of the ejected drops (17).

EHDJ has been investigated with good results to print scaffolds for biological applications. For example Gupta et al. (18) were able to print biodegradable and non-biodegradable nanocomposite scaffolds into pre-designed structures with a thickness limited to five layers of material. EHDJ is gaining even more

interest because it is possible to electrospray viable undamaged mammalian cells. For example Mongkoldhumrongkul et al. (19) performed experiments with EHDJ using a wide range of process parameters showing no significant impact on gene expression, while Clarke et al. (20) demonstrated the ability to electrospray multicellular zebra fish embryos without harmful effects.

EHDJ can also be exploited for the encapsulation of living cells using an alginate solution (21). Alginate is a linear copolymer containing blocks of (1,4)-linked β-d-mannuronic and α-l-guluronics acids. It is a polianionic carbohydrate derived from seaweed, commonly used for encapsulation of living cells (22). It permits the nutrients diffusion and undergoes a sol-gel transition under conditions compatible with cell survival. Multivalent cations (for example Calcium or Barium ions (23,24)) can bind the blocks along the alginate chains, creating ionic bridges, which cause the gelification of aqueous alginate solutions (25,26). Alginate can also be chemically modified to tune its degradation kinetics (27) or can be chemically treated to dissolve and release the entrapped cells (28).

Combining together EHDJ, a computer aided positioning system, an alginate-cell suspension and a proper deposition substrate we believe it is possible to assemble in one single step a cell-laden device/scaffold that can sustain cell survival.

In this article we investigated the possibility to use computer controlled EHDJ printing techniques to obtain depositions of 3D cell laden hydrogels, studying the main process parameters and evaluating the effect of the process itself on cell viability. As a substrate we used gelatin, a thermoresponsive polymer that undergoes a reversible sol-gel transition under 34-36 ℃. Gelatin, being liquid at physiological conditions (29), can be easily removed from the printed sample. Using this hydrogel enriched with calcium ions as bio-paper it was possible to crosslink the alginate bio-ink upon contact onto the substrate, without the need of further processing (30).

2 Materials and Methods

2.1 Materials

Alginic acid sodium salt from brown algae (alginate), calcium chloride dihydrate, low gelling agarose

and gelatin type A (derived from acid-cured porcine skin) were purchased from Sigma-Aldrich (USA). Calcein AM, Propidium Iodide (PI), Phosphate buffer saline without calcium and magnesium (PBS), Dulbecco's modified eagle medium (DMEM) were purchased from Invitrogen (USA). The computer controlled positioning system of the printer is a Janome JR2000N desktop robot (Japan), the deposition system is composed of a high voltage generator (ES30, Gamma High Voltage Research Inc, USA), a pump (NE-300, New Era Pump Systems, USA), a polytetrafluoroethylene tube and a gauge 33 stainless steal needle (outer diameter: 0.210 mm, inner diameter: 0.108 mm Hamilton, Bonaduz/Switzerland). Mouse fibroblasts 3T3 cells line was purchased from the Istituto Profilattico Sperimentale, Brescia, Italy.

2.2 Methods

2.2.1 Preparation and sterilization of alginate, agarose and gelatin

Alginate powder was dissolved in PBS for 8 hours at room temperature under mild stirring to obtain a 2 % alginate solution (2g/100ml). Under a biological sterile hood the solution was loaded into a syringe and capped with a 0.22 μm Luer lock filter. At the other end of the filter a vial was attached and sealed with parafilm. The syringe was placed on an electrical pump set at 10 $\mu L/min$ and the solution was filtered overnight. The sterile solution obtained in the vial was immediately used after filtration. The agarose powder was dissolved under mild stirring in PBS for 3 hours at 60 ℃ to obtain a 2 % agarose solution (2g/100ml). Similarly to the alginate, the agarose solution was filtered but this time the filtration process took place in an oven set at 45 ℃. For the gelatin coating a 400 mM calcium chloride solution was prepared by dissolving the salt in PBS, gelatin powder was added and dissolved under mild stirring condition at 40 ℃ for 3 hours to obtain a 10% gelatin solution (10g/100ml). The filtration process of gelatin was the same as agarose with the oven set at 40 ℃. After filtration the solution in the vial was poured in a 94 mm Petri dish under a biological hood at room temperature, the Petri coated with gelatin was left under the hood for 3 hours to allow the sol-gel transition, 20ml of solution was used for each Petri dish.

2.2.2 Preparation of alginate-cell suspension

The cell culture was performed using standard protocols, in brief about one million of 3T3 mouse fibroblasts cells were thawed and seeded in a 25cm2 flask using DMEM with 2mM Glutamine and 10% Fetal Bovine Serum (Gibco) as culture medium. After 24 h cells were washed in PBS to remove any residues of DMSO left from the freezing solution. At sub confluence (80%) cells were detached from the flask with 0.05 % Trypsin/EDTA (Euroclone) and reseeded in a 175 cm2 flask adding new medium. At confluence cells were detached and moved to a 15 ml vial. Cells inside the vial were stirred at 1000 rounds/min for 10 minutes and the supernatant was removed. Cells on the bottom of the vial were re-suspended in PBS and stirred again to remove any residue of medium containing cations that could crosslink the alginate solution, Cells were dispersed by vibration inside the buffer and an aliquot of the solution was taken to count the cells using a Cellometer Auto T4 and Trypan Blue 0,4% (Invitrogen) as contrast agent. Cells were stirred again, and after removing the supernatant the alginate solution was added to obtain a suspension containing 5 millions cell per milliliter of alginate. Medium, PBS, Trypsin/EDTA and the alginate solution used were previously warmed to 37 ℃.

2.2.3 Printing

The printer (see Figure 1 A) was carefully cleaned with ethanol and placed under a biological hood. It consisted of a positioning and deposition system that can run independently. The programmable positioning system had three degrees of freedom. Samples were placed on a metal base moving linearly (x) while the deposition head was placed above the base, in a plastic holder moving in y and z. The Petri dish, coated with the gelatin hydrogel containing ions, was placed on the metal base of the printer. This metal base was connected to the ground of the generator.

The deposition system consisted of a needle with a custom fit that was placed in the plastic holder of the printer above the base and connected to a polytetrafluoroethylene tube with a Luer lock. The tip of the needle was connected to the positive end of the generator, while the other side of the polytetrafluoroethylene tube was connected to a 3 ml syringe loaded with alginate solution and placed on a pump set to a fixed flux. A calibration was performed for each Petri dish to make the z axis of the printer correspond to zero when the needle was in contact with the gelatin coating. To perform the

experiments the pump was started and the generator was turned on when the solution reached the tip of the needle. This triggered the beginning of the printing program. To remove the samples from the coating, warm DMEM was poured onto the sample and the Petri dish was placed in an incubator at 37 ℃ for few minutes to induce the gel-sol transition of the gelatin. After that, the alginate deposition could be easily removed from the gelatin solution using tweezers, washed again and placed in a flask filled with medium. The flask was placed in the incubator and the medium was changed every day until the end of the experiment.

2.2.4 Agarose mold and alginate dissolution

Some alginate depositions were entrapped in an agarose mold for post processing. At first some agarose was poured to coat the bottom of a 24 wells plate and was left at room temperature to undergo the sol-gel transition. Once the coating was obtained the alginate printed sample was placed on the agarose hydrogel and more liquid agarose was poured in the wells. The samples were left at room temperature until the second layer of agarose became a hydrogel. Samples were removed with tweezers, placed in a 6 well plate containing DMEM and moved in an incubator.

Alginate was dissolved after 6 days of incubation. First the supernatant was removed and the samples were washed with PBS at 37 ℃. A chelating solution containing EDTA was added to remove the crosslinking ions and dissolve the alginate hydrogel. Then the samples were moved to an incubator for twenty minutes to allow the complete dissolution of the gel. Finally, samples in the agarose mold were washed again in PBS, placed in a well plate containing medium and cut with a scalpel to give cells a way out from the hydrogel and observe them re-adhere on the tissue culture plate.

2.2.5 Confocal microscopy

A live/dead assay with Calcein AM and Propidium Iodide was performed on printed hydrogel samples using standard protocols. In brief the samples were moved with tweezers to a new plate containing medium with a 10% v/v Calcein-AM solution, then the well plate was placed in a dark incubator for 30 minutes. At the end of the incubation time the samples were moved to a new well plate and washed three times before adding a 2% v/v Propidium iodide solution. The samples were left for 3 minutes protected from light at room temperature and washed again. All solutions used were at 37 ℃.

Observations with the confocal microscope (Nikon A1, Japan) were performed in wet conditions, a separate image was taken for each setup. Pictures were taken 1 day and 7 days after printing.

3 Results

3.1 Description of printing process

The printing process can be tuned to obtain either single dots or continuous lines. Figure 1 B shows two different kinds of depositions obtained with one single run of the printer. This sample was obtained by programming the printer to perform a 100 mm deposition of alginate on a straight line, then moving back on a parallel path increasing the speed of the needle and the flux of solution, but keeping the distance from target and applied voltage constant. Alginate undergoes a fast sol-gel transition upon contact to the gelatin hydrogel containing calcium cations so that a hydrogel immediately forms. The drops ejected from the needle, as a result from the impact on the substrate, squeeze on the coating losing their spherical shape; this is clear if the width of the sample is compared to its thickness (the side view of the continuous deposition is shown in Figure 1 C). Subsequently the cations diffuse in the alginate leading to a complete sol-gel transition of the whole bead. The straight line results from the coalescence of closed packed beads, as evidenced in the optical microscope image in Figure 1D where the boundaries between the beads can be recognized.

Similarly to gelatin, alginate hydrogel can act itself as a source of crosslinking ions. This permits obtaining thick samples with a layer-by-layer deposition. In fact the top layer can crosslink thanks to the ions coming from the substrate below, being it gelatin or a previously printed alginate layer. Anyway the printing speed has to match the diffusion rate, which will decrease with the thickness of the construct. The thicker the deposition is, the more time is needed to obtain a sol-gel transition of the last deposited layers. For these reasons a pause could be necessary after each layer, in case that the ions diffusion speed is not sufficient to fully gelify the alginate. This is particularly evident for small samples where the layer trajectory is short and it is necessary to pause the process to avoid the deposition of alginate solution on top of a still partially liquid layer of alginate. If the sample is big enough and, as such, the printer takes more time to complete each layer, this pause is not necessary.

Moreover once the generator is turned on a short time is needed to establish a regular jet of drops, so it is not possible to predict when the first drop will be ejected from the needle. For this reason it was convenient to plan the deposition including an extra trajectory to build up a sacrificial part to be easily removed at the end of the printing process. Figure 2 shows parts of the procedure to obtain a small multi layered cylindrical structure with a radius equal to 1.5 mm (distance from the center of the cylinder to the center of the deposition, estimated error of 10%). First the needle slowly moved in a "standby area" (zone between points 1 and 2) to allow enough time for the sol-gel transition of the previously deposited layers. Then it rapidly accelerated in a zone between points 2 and 3 to limit material deposition and facilitate the removal from the final construct. Once in the deposition zone (circular ring after point 3), speed was set for optimal deposition. Full 3D fabrication can be obtained by overlapping multiple layers, repeating the procedure and progressively increasing the "z" coordinate of the needle. By following this procedure it was possible to print structures up to 2 mm height, enough to allow an easy addition of a solution of calcium enriched gelatin to the side and into the middle of the sample. By adding more gelatin it is possible to sustain more layers and as such to sustain taller structures. This way the potential limit of calcium diffusion inside the gel can be overcome. A similar microfabricted structure was proposed by Teramura et al. to build macrocapsule loaded with Langerhans islets as an artificial pancreas (31).

3.2 Process parameters

The EHDJ printing process is influenced by parameters such as the flux of solution flowing through the needle, the potential applied, the speed of the needle in the x and y plane and the distance between the tip of the needle and the top of the gelatin coating underneath it. The speed of the needle was found to have a strong influence on the characteristics of the printed samples so we tested all the aforementioned parameters versus speed, ranging from 1 to 6 mm/s. As a starting set up we printed samples at 14KV, 10 $\mu L / min$ at a distance of 5 mm varying one single parameter for each experiment.

3.2.1 Flux of solution vs speed

By increasing the flux of solution from 5 to 10 and 20 $\mu L / min$ more deposition were continuous and thicker, Figure 3. At 5 $\mu L / min$ the tendency was to obtain dotted depositions, partially bridged together at low speeds. At 20 $\mu L / min$ the tendency was opposite and more continuous deposition

could be obtained with only one dotted printed line at the highest speed tested (6 mm/s). At 10 $\mu L/min$ the depositions were continuous at lower speeds, while becoming aligned dots at higher speeds. All the tested samples did not present any deviations from a straight line. For each set of samples it was possible to observe an inverse relation between the speed of the needle and the diameter of the deposition, with thinner depositions obtained at higher speeds. Together, as expected, depositions were generally thicker at higher fluxes. For example it was possible to observe dots with a diameter of 298 ± 5 μm at 5 $\mu L/min$ and 6 mm/s speed increasing up to almost 600 μm when the flow of solution was set at 20 $\mu L/min$.

3.2.2 Voltage vs speed

The tested voltages ranged between 12 to 20 KV with increments of 2 KV. At 12KV a proper jet of drops could not be established as shown in Figure 4: single beads were deposited by gravitational dripping and they were closer to each other at lower speed. From 14 KV up the jet of drops could be established. By further increasing the voltage a certain degree of disorder appeared on the printed samples. At 20KV the voltage was too high to obtain an ordered deposition, with all the deposition lines resulting misaligned and irregular.

3.2.3 Distance from target vs speed

The tested distances from target ranged between 4 and 7 mm, Figure 5. At 4 and 5 mm results were quite similar, with two continuous lines in each sample at 1 and 2mm/s and dotted lines at higher distances. All 12 depositions (either continuous or dotted lines) were uniform and straight. By increasing the distance from target over 5 mm the beads ejected from the needle tended to aggregate in spots, leading to deposition lines with a diameter that changed along the deposition path. At 7 mm it was possible to observe evident deviations from a straight line. For distances under 4 mm the tip of the needle was too close to the gelatin target and causing sparks generation, thus inhibiting the formation of the jet.

3.3 Printed samples with cells

Samples were realized setting the printing apparatus to the best working conditions. The voltage was set at 14KV because it was the only value giving straight deposition lines of beads among the five tested. The flux of solution was set to $10 \mu L / min$, being the best balance between throughput and spot size. The distance from the target was set at 5 mm that, together with 4 mm, gave the best uniform and straight deposition. The needle speed along the x, y plane, a parameter that doesn't affect cells, was arbitrary chosen at 4 mm/s. An alginate suspension containing $5x10^6$ cells /ml was used. All samples were made of 5 layers and printed on a gelatin coated Petri dish.

Samples were cultured for 1 and 7 days before observing them with the confocal microscope after Calcein AM and Propidium Iodide staining. As shown in Figure 6 in both cases they were able to maintain entrapped cells viable and evenly distributed.

Some samples were molded in agarose to show that cells retain the ability to expand once released from the printed alginate. In this case the alginate was dissolved at day 6 and, after being cultured for one more day on a tissue culture plate, they were observed with confocal and optical microscope. As shown in Figure 7 the dissolution of the alginate was effective and cells, without the matrix supporting them, lost their 3 dimensional distribution. Cells formed a two dimensional layer at the base of the volume left from the dissolved alginate. When the mold was cut, cells from this layer were able to move outside and re-adhere on the tissue culture plate.

4 Discussion

It is generally difficult to predict quantitatively the outcome of electro hydro dynamic processes. For example, by changing the concentration of a biomaterial in solution, the electrical and rheological properties of the solution change affecting the outcome of the process. Similarly, changing the printing parameters such as voltage, flux of solution leads to differently printed samples. Some mathematical models of the described process exist, but their application is not immediate for a non Newtonian fluid (alginate) containing particles (cells). However general qualitative information can be drawn (32) by observing the samples obtained with the printer.

Considering the voltage, it was possible to initiate the jetting condition starting from 14 kV. Below this value we observed only the acceleration of the dripping rate from the syringe, without any effect on the diameter of the drops. It should be noted that, with our setup, higher voltages were needed to obtain a jetting conditions, compared to data found in literature regarding cell encapsulation experiments using EHDJ (6 - 7 KV)(33). In these experiments beads are ejected directly in a calcium chloride bath, while in our setup beads were ejected onto a gelatin hydrogel. We believe that the presence of the gelatin between the cathode and the anode mitigates the effect of the applied voltage. In fact it was observed that the jetting condition can be initiated only at a certain distance from the gelatin substrate, while, moving the needle closer, it suddenly stops, to start again after the gelatin was removed.

With the voltage set at 14 kV the depositions obtained were straight and uniform. By increasing the voltage, the depositions were less uniform. At 14 KV and needle speed of 6 mm/s (Figure 4) the average diameter was 450 $\pm$ 16 μm while at 20 KV it was 268 $\pm$ 75 μm. At 20 KV the average diameter was smaller, but the dispersion was higher. In fact it was possible to observe the presence of much smaller beads. This observation is consistent with the results obtained by Hayati et al.(34) who showed a decrease in the average diameter of the jet with increasing voltages. Moreover, as suggested by Cloupeau et al.(35), a high voltage can generates an unstable Taylor cone and secondary disintegration, leading to beads characterized by a small size and high dispersion.

In EHD processes the flux of solution, as observed by Hwang et al. (36), plays a crucial role, with higher fluxes generating bigger beads and as such bigger building blocks. In the EHDJ printing a high flux of solution is necessary to obtain a high throughput but this leads to thicker depositions and, consequently, to a lower printing resolution. For example (Figure 3) with a flux of solution of 20 $\mu L/min$ and a needle speed of 1mm/s the average diameter was about 960 $\pm$ 120 μm, while at 5 $\mu L/min$ the average diameter of the deposition was 512 $\pm$ 68 μm. On the other side it was possible to partially mitigate this phenomenon by increasing the speed of the needle, in fact at 3 mm/s and a flux of 20 $\mu L/min$ the average diameter became 598 $\pm$ 59 μm.

Shorter distances are generally preferred since the droplets, once ejected, are subjected to perturbations that influence their trajectory, leading to placement errors (16). In fact at higher distances the deposition appeared less regular. For EHDJ printing, typical working distances found in literature are in the sub-

micrometric range (37) but typically the samples are printed on top of a dry substrate like a silicon wafer. If the distance is too short, electric discharge occurs, with the formation of an electrical arc between the needle and the substrate. In our experiment (using a water based solution printed on top of a substrate with high water content) the minimum working distance possible was 4 mm. This means that at short distances (3mm) it was not possible to overcome the Rayleigh that determines the jetting condition because of the formation of the arc itself.

In our setup the best distance possible was found to lie between 4 and 5 mm (both settings gave similar results). When the distance of the needle from the substrate was higher, the drops showed an elliptical shape once deposited on the substrate. For example (Figure 5) at 5 mm and with a speed of the needle of 6 mm/s the ratio between the major and the minor axis was between 1 and 1.2 for most of the observed drops while at a 7 mm the range increased up to 1.8.

Other parameters characterizing the process like polymer concentration, density of cells and diameter of needle and their effect on the EHDJ process were previously characterized (38). In brief the density of cells in the starting solution influenced the EHDJ process, for example solutions with higher cell densities ($10-20\times10^6$ cells/ml) needed a higher voltage to establish a jet of drops. However once the jet of drops was established there were no substantial differences on the diameter of the ejected beads. The diameter of the needle was chosen to match the best compromise between viscosity and printer spot size, since higher diameter allow higher solution flux, but increased the spot size of the printer, creating bigger beads. The best alginate solution concentration was found to be 2%. Higher concentrations were possible, but the increase of viscosity had to be balanced by decreasing the flux of solution. On the other hand lower concentration were problematic because lower intermolecular cohesive interactions led to secondary disintegration of the jet and, as such, to irregular depositions. Once the concentration of alginate was set at 2%, we empirically found that the optimal concentration of calcium chloride to obtain thicker multi layer samples was 400mM. In fact, according to results found in literature (39,40), when a solution of alginate is placed in contact with calcium chloride higher concentrations of salt solution favor the diffusion of the solute and, thus, the formation of thicker hydrogels. Furthermore faster gelation times are obtained using higher concentrations of divalent cations in solution. The concentration of calcium ions we used was higher than the physiological one and this may affect cells. It should be noted that the

printing procedure was relatively fast but further studies may be needed to assess the effect of such calcium concentration on cell behavior.

Cell viability was evaluated by means of confocal microscopy. We did not observe substantial differences between samples at day 1 and samples at 7 days in terms of number of living cells. This is partially expected and can be explained considering that the proliferation of anchorage dependent cells, such as fibroblasts, is inhibited in alginate since it does not present adhesion motifs and its hydrophilic nature discourage the adsorption of cell adhesion proteins (25). This observation is consistent with the results obtained by Ma et al. (41) who showed that cells in alginate microcapsules are in a semi-quiescent state. They observed a marked increase in the percentage of cells in G0G1 phase together with a decrease in the percentage of cells in S and G2M phases. For applications where cell adhesion and matrix degradation are needed, alginate can be modified to tune its degradation kinetics (42,43) and to include cell adhesion motifs. For example Yu et al. (44) demonstrated that RGD peptides conjugated to alginate improved human umbilical vein endothelial cell adhesion and proliferation when compared to an unmodified control. The results of our observation by confocal microscope were also consistent with our previous observations on cells encapsulated by EHDJ that showed a low number of dead cells up to 30 days after encapsulation (38). This suggests, as initially hypothesized, that the EHDJ technology to encapsulate cells can be safely transferred to a bioprinter and assemble in one single step cell laden devices/scaffolds that can sustain cell survival.

In Table 1 we report some features of the printer used in these experiments and compared them to other printing system found in scientific literature (13). This table collects only the few features reported for these printers. For example does not take into account the ability to print directly 3D structures that, in some cases, is missing. Being bioprinting a relatively new technology, it is not yet clear which printing systems among these is best suited for a specific application. In fact the aforementioned printers have been used for a wide variety of application using different kind of cells like neurons, fibroblasts, endothelial and stem cells (45–47). In the ink-jet and syringe extrusion printers a fluid is forced out of an orifice, typically smaller than 100 μm, creating droplets of 300 μm or more. The droplets size is comparable to that of the EHDJ printer (9) suggesting that these printers may be characterized by a similar resolution. By the way the high voltage driving technology may also be improved to reduce the

final spot size, accordingly to results found in literature, and, as such, to obtain much higher resolutions (48). A clear advantage of using EHDJ printers, when compared to ink-jet printers, is the fact that they can be used for processing a wider range of suspensions. In particular they can be tuned for highly concentrated suspensions (high material loading/high cell density) at the "small" price of a reduced throughput (49). In spite of some limitation, ink-jet printers rely on a cheap but advanced and established technology developed for desktop printers that allow, for example, to use four different materials or suspensions at the same time (corresponding to the RGB and black reservoirs for the ink) and manufacture more complex, biomimetic samples. On the opposite side laser printers are the most complex printers among the available technologies. In laser printers, an electromagnetic beam with a diameter width of few microns induce the transfer of cells from specifically engineered substrates to a close target, creating droplets of cells smaller than 100 μm. The target is coated with a hydrogel to avoid drying effects and excessive shear forces (50) and 3D printing is usually obtaining by transferring one or few layers of cells and coat them with new hydrogel. These printers are characterized by high resolutions that allow the precise patterning of single cells to manufacture complex structures. These kinds of resolutions are difficult to be obtained by other printing techniques, making laser printers ideal candidates when high resolutions are needed (e.g. complex microvascular structures). On the other side, considering the setup of these printers, to obtain 3D structures bigger than few layers of cells may be more challenging. The maximum cell throughput of EHDJ printing is among the highest of the printers reported in literature. The loaded volume of the printer depends on the syringe used on the pump that can mount up to 50 ml syringes. This high load volume, not available in all other systems, allows uninterrupted printing for extended periods of time. Another aspect not present in all other printers is that the part of deposition system on top of the bio-paper is small, being constituted of simple and low cost components: a needle, a cable and a tube. The most expensive element of the deposition system is the high voltage generator, which is however a common component available in many research laboratories. Furthermore EHDJ printer can work on samples that are not perfectly planar because there is a 1 mm range of suitable operating distances, easing the complexity of a precise z mapping of the substrate.

In this proof of concept study, alginate was used as a bio-ink because it is widely used for cell encapsulation and it is characterized by a fast sol-gel transition. In fact when a drop of alginate reaches

the target, divalent cations crosslink the surface of the alginate solution in contact with the substrate, locally increasing its viscosity and practically "gluing" the drop on the target. We believe that this printing technique could be applied also to other materials like photo-cross-linkable hydrogels. There are many examples of these polymers used for cell encapsulation such as blends of poly (ethylene oxide) and poly (ethylene oxide) dimethacrylate (51) and RGD incorporating poly(ethylene glycol) diacrylate (52) . Some of these polymers can form a jet of beads (53) and in some cases the sol-gel transition is relatively fast (15 seconds (54)), making them potential candidates to be used as bio-ink for an EHDJ printing technique targeted at specific applications.

Overall, EHDJ printing is a technique capable to create viable cells containing 3D structures and it has the potential to be considered as a valid alternative to more established bioprinting methods. Further work is required to adapt this technique to specific applications, where different combinations of bio-inks and bio-paper may be need. An example is the possibility to realize a nerve conduit by integrating a hollow cylindrical scaffold containing glial cells able recreate a suitable chemical environment, a physical constrain and a guide for axon regrowth in the cavity (55,56). Another possibility deals with the realization of pancreatic islets loaded devices, able to release insulin as a response to glucose concentration (6,31).

5 Conclusions

In this study we demonstrated that the electrohydrodynamic process can be exploited as the deposition system to print alginate hydrogels containing living cells. By optimizing the printing parameters it is possible to obtain and control a jet of alginate beads that can be placed precisely on a target substrate. If the surface is a hydrogel containing divalent cations the alginate crosslinks upon contact without the need of further processing. The printing process is compatible with cell survival and allows the deposition of three-dimensional constructs. The ability to build such constructs could facilitate the design and manufacturing of scaffolds with predefined 3 dimensional shapes that may find significant applications in the field of tissue engineering

6 Acknowledgment

This research was done thanks to Biotools srl (a spin-off of the University of Trento - Italy) that lent the desktop robot.

References

1. Mironov V, Visconti RP, Kasyanov V, Forgacs G, Drake CJ, Markwald RR. Organ printing: tissue spheroids as building blocks. Biomaterials. **30**(12), 2164, 2009;

2. Bhadriraju K, Chen CS. Engineering cellular microenvironments to improve cell-based drug testing. Drug Discov. Today. **7**(11), 612, 2002;

3. Elbert DL. Bottom-up tissue engineering. Curr. Opin. Biotechnol. **22**(5), 674, 2011;

4. Khademhosseini A, Langer R. Microengineered hydrogels for tissue engineering. Biomaterials. **28**(34), 5087, 2007;

5. Dimitrov DS. Therapeutic proteins. Methods Mol. Biol. **899**, 1, 2012;

6. De Vos P, Faas MM, Strand B, Calafiore R. Alginate-based microcapsules for immunoisolation of pancreatic islets. Biomaterials. **27**(32), 5603, 2006;

7. Murua A, Orive G, Hernández RM, Pedraz JL. Xenogeneic transplantation of erythropoietin-secreting cells immobilized in microcapsules using transient immunosuppression. J. Control. Release. **137**(3), 174, 2009;

8. Chang P. The in vivo delivery of heterologous proteins by microencapsulated recombinant cells. Trends Biotechnol. **17**(2), 78, 1999;

9. Xu T, Jin J, Gregory C, Hickman JJJJ, Boland T. Inkjet printing of viable mammalian cells. Biomaterials. **26**(1), 93, 2005;

10. Cui X, Boland T. Human microvasculature fabrication using thermal inkjet printing technology. Biomaterials. **30**(31), 6221, 2009;

11. Barron JA, Wu P, Ladouceur HD, Ringeisen BR. Biological Laser Printing: A Novel Technique for Creating Heterogeneous 3-dimensional Cell Patterns. Biomed. Microdevices. **6**(2), 139, 2004;

12. Ringeisen BR, Kim H, Barron JA, Krizman DB, Chrisey DB, Jackman S, et al. Laser printing of pluripotent embryonal carcinoma cells. Tissue Eng. **10**(3-4), 483, 2004;

13. Ringeisen BR, Othon CM, Barron J a, Young D, Spargo BJ. Jet-based methods to print living cells. Biotechnol. J. **1**(9), 930, 2006;

14. Bock N, Dargaville TR, Woodruff M a. Electrospraying of polymers with therapeutic molecules: State of the art. Prog. Polym. Sci. **37**(11), 1510, 2012;

15. Taylor G. Disintegration of water drops in electric field. Proc. R. Soc. London. **280**(1380), 383, 1964;

16. Park J-U, Hardy M, Kang SJ, Barton K, Adair K, Mukhopadhyay DK, et al. High-resolution electrohydrodynamic jet printing. Nat. Mater. **6**(10), 782, 2007;

17. Moghadam H, Samimi M, Samimi A, Khorram M. Electrospray modeling of highly viscous and non-Newtonian liquids. J. Appl. Polym. Sci. **118**(3), 1288, 2010;

18. Gupta A, Seifalian AM, Ahmad Z, Edirisinghe MJ, Winslet MC. Novel Electrohydrodynamic Printing of Nanocomposite Biopolymer Scaffolds. J. Bioact. Compat. Polym. **22**(3), 265, 2007;

19. Mongkoldhumrongkul N, Best S, Aarons E, Jayasinghe SN. Bio-electrospraying whole human blood : analysing cellular viability at a molecular level. J. Tissue Eng. Regen. Med. **3**(June), 562, 2009;

20. Clarke JDW, Jayasinghe SN. Bio-electrosprayed multicellular zebrafish embryos are viable and develop normally. Biomed. Mater. **3**(1), 011001, 2008;

21. Xie J, Wang C-H. Electrospray in the dripping mode for cell microencapsulation. J. Colloid Interface Sci. **312**(2), 247, 2007;

22. Murua A, Portero A, Orive G, Hernández RM, de Castro M, Pedraz JL. Cell microencapsulation technology: Towards clinical application. J. Control. Release. **132**(2), 76, 2008;

23. Peirone M, Ross CJ, Hortelano G, Brash JL, Chang PL. Encapsulation of various recombinant mammalian cell types in different alginate microcapsules. J. Biomed. Mater. Res. **42**(4), 587, 1998;

24. Duvivier-Kali VF, Omer A, Parent RJ, O'Neil JJ, Weir GC. Complete Protection of Islets Against Allorejection and Autoimmunity by a Simple Barium-Alginate Membrane. Diabetes. **50**(8), 1698, 2001;

25. Rowley JA, Madlambayan G, Mooney DJ. Alginate hydrogels as synthetic extracellular matrix materials. Biomaterials. **20**(1), 45, 1999;

26. Lee KY, Mooney DJ. Alginate: Properties and biomedical applications. Prog. Polym. Sci. **37**(1), 106, 2012;

27. Yang J-S, Xie Y-J, He W. Research progress on chemical modification of alginate: A review. Carbohydr. Polym. **84**(1), 33, 2010;

28. Siti-Ismail N, Bishop AE, Polak JM, Mantalaris A. The benefit of human embryonic stem cell encapsulation for prolonged feeder-free maintenance. Biomaterials. **29**(29), 3946, 2008;

29. Klouda L, Mikos AG. Thermoresponsive hydrogels in biomedical applications. Eur. J. Pharm. Biopharm. **68**(1), 34, 2008;

30. Pataky K, Braschler T, Negro A, Renaud P, Lutolf MP, Brugger J. Microdrop Printing of Hydrogel Bioinks into 3D Tissue-Like Geometries. Adv. Mater. **24**(3), 391, 2011;

31. Teramura Y, Iwata H. Bioartificial pancreas microencapsulation and conformal coating of islet of Langerhans. Adv. Drug Deliv. Rev. **62**(7-8), 827, 2010;

32. Jacobs V, Anandjiwala RD, Maaza M. The influence of electrospinning parameters on the structural morphology and diameter of electrospun nanofibers. J. Appl. Polym. Sci. **115**(5), 3130, 2010;

33. Manojlovic V, Djonlagic J, Obradovic B, Nedovic V, Bugarski B. Investigations of cell immobilization in alginate: rheological and electrostatic extrusion studies. J. Chem. Technol. Biotechnol. **81**(4), 505, 2006;

34. Hayati I, Bailey A, Tadros T. Investigations into the mechanisms of electrohydrodynamic spraying of liquids: I. Effect of electric field and the environment on pendant drops and factors affecting the. J. Colloid Interface Sci. **117**(1), 205, 1987;

35. Cloupeau M, Prunet-Foch B. Electrohydrodynamic spraying functioning modes: a critical review. J. Aerosol Sci. **25**(6), 1021, 1994;

36. Jun Y, Kim MJ, Hwang YH, Jeon EA, Kang AR, Lee S-H, et al. Microfluidics-generated pancreatic islet microfibers for enhanced immunoprotection. Biomaterials. **34**(33), 8122, 2013;

37. Choi HK, Park J-U, Park OO, Ferreira PM, Georgiadis JG, Rogers J a. Scaling laws for jet pulsations associated with high-resolution electrohydrodynamic printing. Appl. Phys. Lett. **92**(12), 123109, 2008;

38. Gasperini L, Maniglio D, Migliaresi C. Microencapsulation of cells in alginate through an electrohydrodynamic process. J. Bioact. Compat. Polym. **28**(5), 413, 2013;

39. Kuo CK, Ma PX. Ionically crosslinked alginate hydrogels as scaffolds for tissue engineering: Part 1. Structure, gelation rate and mechanical properties. Biomaterials **22**(6), 511, 2001;

40. Blandino ANA, Macias M, Canter D. Formation of Calcium Alginate Gel Capsules : Influence of Sodium Alginate and CaC12 Concentration on Gelation Kinetics. **88**(6), 686, 1999;

41. Ma H-L, Hung S-C, Lin S-Y, Chen Y-L, Lo W-H. Chondrogenesis of human mesenchymal stem cells encapsulated in alginate beads. J. Biomed. Mater. Res. A. **64**(2), 273, 2003;

42. Bouhadir KH, Lee KY, Alsberg E, Damm KL, Anderson KW, Mooney DJ. Degradation of partially oxidized alginate and its potential application for tissue engineering. Biotechnol. Prog. **17**(5), 945, 2001;

43. Gomez C, Rinaudo M, Villar M. Oxidation of sodium alginate and characterization of the oxidized derivatives. Carbohydr. Polym. **67**(3), 296, 2007;

44. Yu J, Gu Y, Du KT, Mihardja S, Sievers RE, Lee RJ. The effect of injected RGD modified alginate on angiogenesis and left ventricular function in a chronic rat infarct model. Biomaterials. **30**(5), 751, 2009;

45. Tasoglu S, Demirci U. Bioprinting for stem cell research. Trends Biotechnol. **31**(1), 10, 2013;

46. Boland T, Xu T, Damon B, Cui X. Application of inkjet printing to tissue engineering. Biotechnol. J. **1**(9), 910, 2006;

47. Mironov V, Kasyanov V, Markwald RR. Organ printing: from bioprinter to organ biofabrication line. Curr. Opin. Biotechnol. **22**(5), 667, 2011;

48. Derby B. Printing and prototyping of tissues and scaffolds. Science. **338**(6109), 921, 2012;

49. Jayasinghe SN, Qureshi AN, Eagles PAM. Electrohydrodynamic jet processing: an advanced electric-field-driven jetting phenomenon for processing living cells. Small. **2**(2), 216, 2006;

50. Schiele NR, Corr DT, Huang Y, Raof NA, Xie Y, Chrisey DB. Laser-based direct-write techniques for cell printing. Biofabrication. **2**(3), 032001, 2010;

51. Elisseeff J, McIntosh W, Anseth K, Riley S, Ragan P, Langer R. Photoencapsulation of chondrocytes in poly(ethylene oxide)-based semi-interpenetrating networks. J. Biomed. Mater. Res. **51**(2), 164, 2000;

52. Yang F, Williams CG, Wang D-A, Lee H, Manson PN, Elisseeff J. The effect of incorporating RGD adhesive peptide in polyethylene glycol diacrylate hydrogel on osteogenesis of bone marrow stromal cells. Biomaterials. **26**(30), 5991, 2005;

53. Morota K, Matsumoto H, Mizukoshi T, Konosu Y, Minagawa M, Tanioka A, et al. Poly(ethylene oxide) thin films produced by electrospray deposition: morphology control and additive effects of alcohols on nanostructure. J. Colloid Interface Sci. **279**(2), 484, 2004;

54. Cruise GM, Hegre OD, Scharp DS, Hubbell J a. A sensitivity study of the key parameters in the interfacial photopolymerization of poly(ethylene glycol) diacrylate upon porcine islets. Biotechnol. Bioeng. **57**(6), 655, 1998;

55. Francisco H, Yellen BB, Halverson DS, Friedman G, Gallo G. Regulation of axon guidance and extension by three-dimensional constraints. Biomaterials. **28**(23), 3398, 2007;

56. Schnell E, Klinkhammer K, Balzer S, Brook G, Klee D, Dalton P, et al. Guidance of glial cell migration and axonal growth on electrospun nanofibers of poly-ε-caprolactone and a collagen/poly-ε-caprolactone blend. Biomaterials. **28**(19), 3012, 2007;

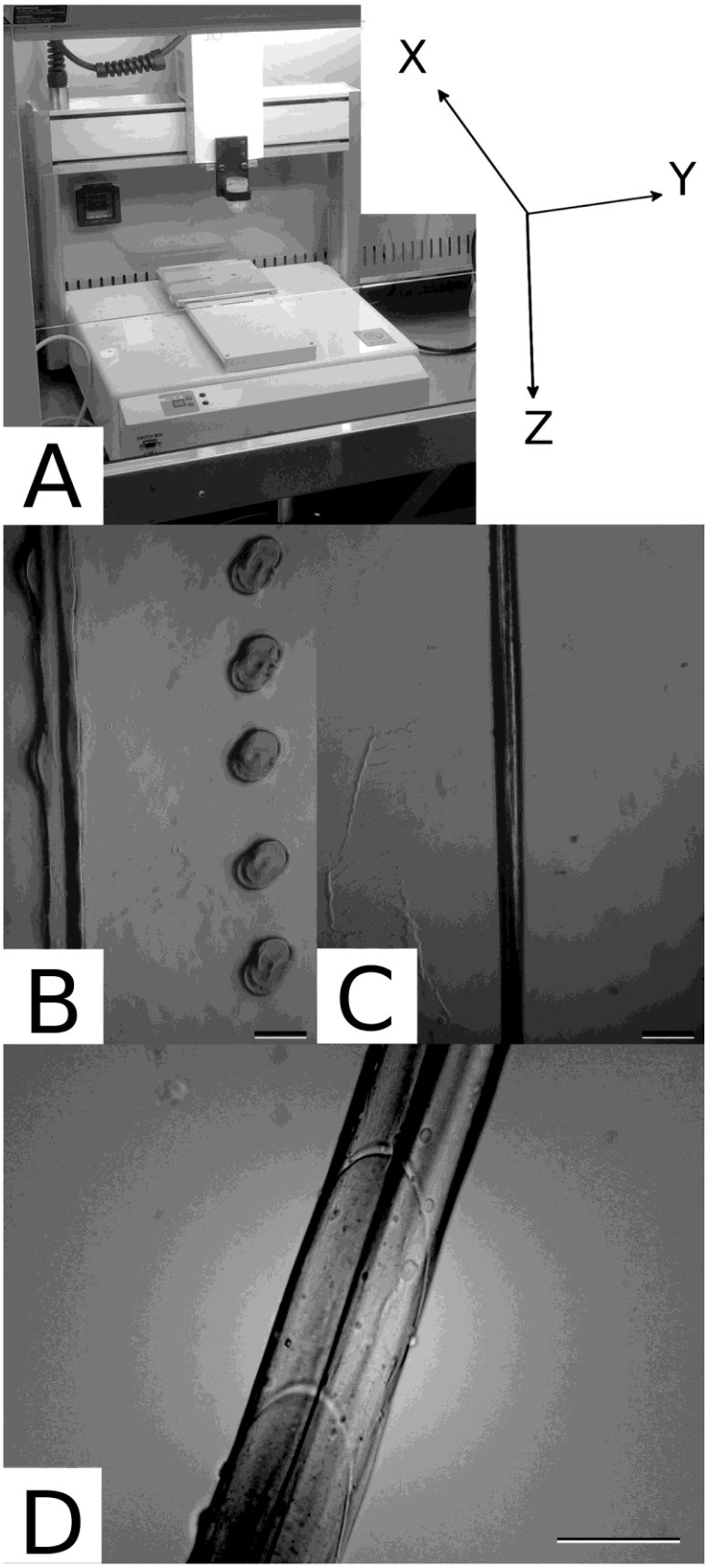

Figure 1: Deposition of alginate A) the printer, B) two different kinds of deposition by changing the speed of the needle, view from top, C) view from side of the continuous line deposition D) beads that coalesce together to create a continuous line. Bar is 500 μm

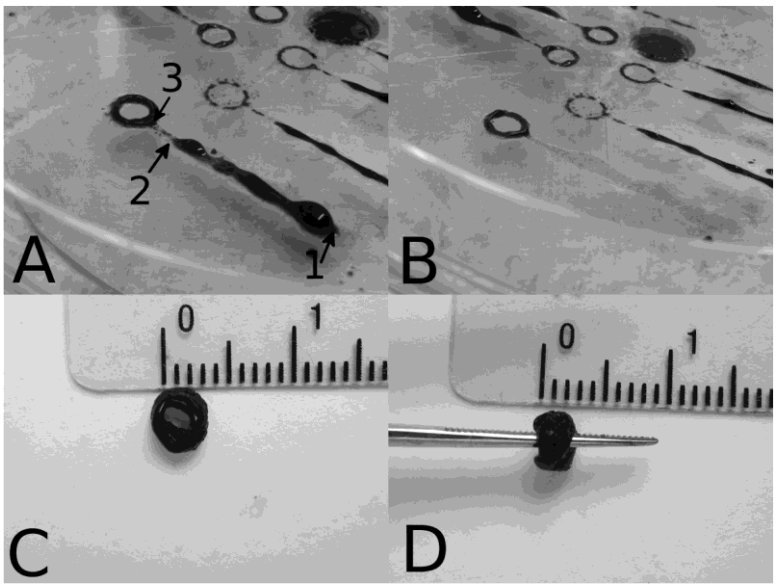

Figure 2: Printing a “small thick sample”, A) initial deposition design with sacrificial part B) sample with sacrificial part removed C and D) sample after some layers of deposition.

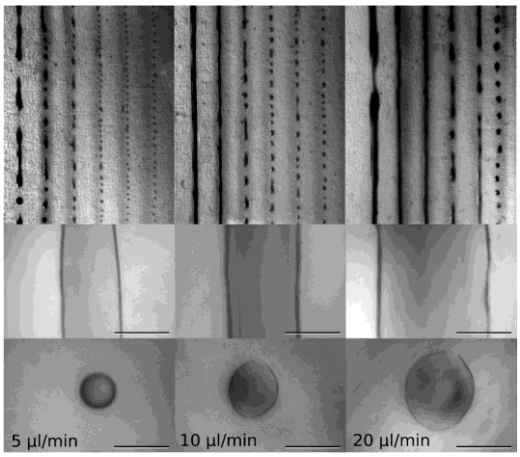

Figure 3: From left to right depositions at 5 µL/min, 10 µL/min, 20 µL/min. Top row shows the geometrical feature of the depositions varying the needle speed from 1 to 6 mm/s. Middle row shows depositions obtained at 1 mm/s while bottom row shows depositions at 6 mm/s. Scale bar is 500 µm

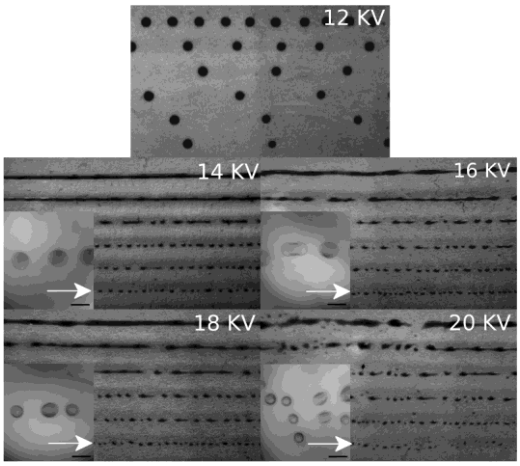

Figure 4: Each of the 5 pictures shows the geometrical feature of the depositions varying the needle speed from 1 (top) to 6 mm/s (bottom). Magnification shows depositions obtained at 6 mm/s. Bar is 500 μm

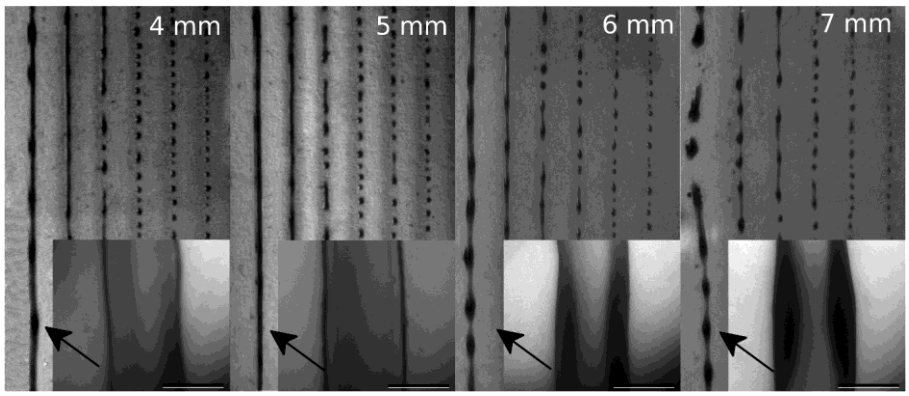

Figure 5: From left to right depositions at a distance of 4, 5, 6, 7 mm. Each of the four images shows the geometrical feature of the depositions varying the needle speed from 1 (left) to 6 (right) mm/s. Picture insets refer to the depositions obtained at 1 mm/s. Bar is 500 μm

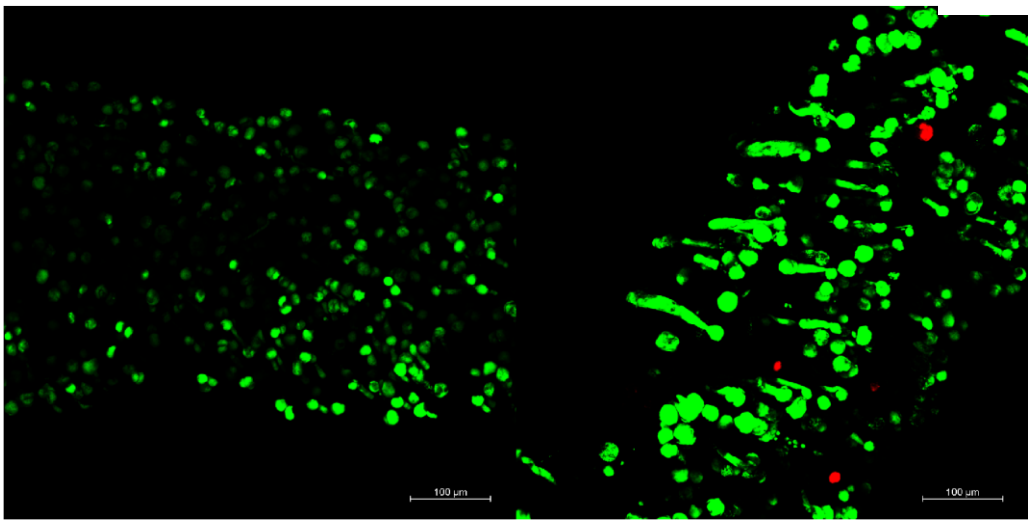

Figure 6: Deposition of cell laden alginate after 1 day (left) and 7 days of culture (right), confocal microscopy live/dead assay (green/red) with Calcein AM and Propidium Iodide. Bar is 100 µm

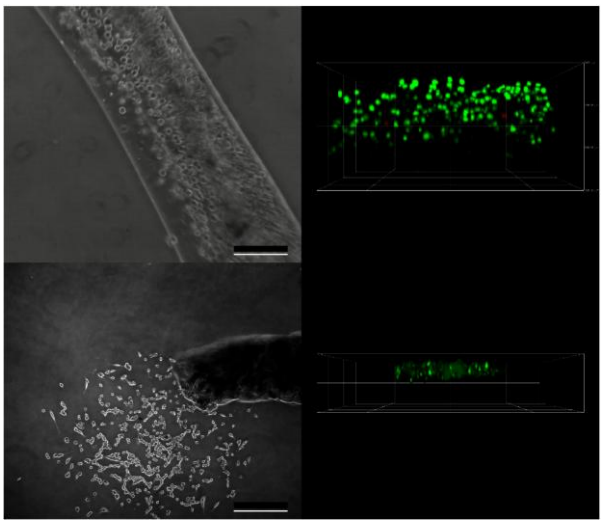

Figure 7: Optical (left) and confocal (right) images of alginate deposition after 7 days from cells encapsulation. Confocal images after Calcein AM and Propidium Iodide staining showing living (green) and dead cells (red). Upper left) optical microscope image of alginate-cell suspension. Upper right) 3D confocal image of alginate deposition after 7 days from deposition showing the distribution of cells inside the alginate, green spots are living cells. Bottom left optical microscope image of cells outside the agarose mold and re-adhering on the tissue culture plate. Bottom right) 3D confocal image of the agarose mold taken after 7 days from deposition showing that the dissolution method was effective in removing the alginate matrix that sustained the cells, green spots are living cells. Bar is 250 μm

	Spot size (μm)	Max cell throughput (cells/s)	Loaded volume (ml)	Cell viability (%)
EHDJ	>300	1600 (6000*)	depends on syringe used	>95
Laser Guided Direct Write	30	0.04	Not reported	Not reported
Modified Laser Induced Forward Transfer	30-100	10^4	0.02	>95
Inkjet - Thermal	>300	850	0.3 - 0.5	75 - 90
Inkjet - Piezo	Not reported	2	0.3 - 0.5	Not reported
Syringe Extrusion	>300	Not reported	0.6	>90

Table 1: Features of the printer system reported (gray background) compared to other printers found in literature [13] (white background). * Tested but not reported